Least-Squares Method for Quantitative Determination of Chemical Exchange and Cross-Relaxation Rate Constants from a Series of Two-Dimensional Exchange NMR Spectra

Zsolt Zolnai,[†] Nenad Juranić, and Slobodan Macura*

Department of Biochemistry and Molecular Biology, Mayo Clinic and Foundation, Mayo Graduate School, Rochester, Minnesota 55905

Received: December 3, 1996; In Final Form: March 13, 1997[⊗]

We present a new method, the least-error matrix analysis (LEMA), to quantify the dynamic matrix from a series of 2D NMR exchange spectra. The method is based on a weighted averaging of individual dynamic matrices. The matrices are obtained by full-matrix analysis (FMA) from a series of 2D exchange spectra recorded at different mixing times. The weights, calculated by error propagation analysis, are explicit functions of the mixing time. The principal advantage of LEMA in comparison to FMA is that it uses all the known relationships between the spectral peaks: the peak correlations within 2D spectra, and the mixing time evolution among the spectra. We tested LEMA by analyzing a series of 10 cross-relaxation spectra (NOESY, $\tau_m = 60$ μs−1.28 s) in a rigid 10-spin system (cyclo(L-Pro-Gly) in 3:1 v/v H_2O/DMSO). At 233 K the dipeptide has a mobility like a small protein with a correlation time of 3.8 ns. While FMA at $\tau_m = 30$ ms could extract only 14 distances in a range 1.75−3 Å, LEMA provided 22 distances, of which the longest was 4 Å. The extension of the available interproton distances from 3 to 4 Å afforded by LEMA is caused by a 10-fold decrease of the lower limit of measurable cross-relaxation rates, from −0.59 to −0.06 s^{-1}. The most important property of LEMA, provision of accurate average values of magnetization exchange rates from a given set of peak volumes, is verified experimentally on a model system.

Introduction

The most notable forms of two-dimensional (2D) NMR exchange spectroscopy[1] that contributed immensely to the popularity of 2D NMR method in chemistry[2] are the chemical exchange spectroscopy (EXSY)[3,4] and nuclear Overhauser enhancement spectroscopy (NOESY).[5,6] A particularly impressive application of NOESY is the determination of the solution structure of proteins.[7] Although a semiquantitative analysis was typically used for it, it is well recognized that the quantitative analysis of cross-relaxation spectra might be more useful.[8−16] Similarly, the quantification of EXSY spectra improves their utility to study chemically exchanging systems.[17−21] However, only a few attempts have been made to estimate the corresponding error limits.[19,22−27]

The determination of the magnetization exchange rate constants $[\boldsymbol{L}]_{pq}$ is independent from the type of exchange observed (cross-relaxation in NOESY, or chemical exchange in EXSY), since both transfer types are directed by the same master equation. The methods to quantify exchange spectra can be roughly divided into two categories: buildup rate analysis (BU)[6,28] and full-matrix analysis (FMA).[8,11,13] The BU analysis provides the $[\boldsymbol{L}]_{pq}$'s from the time evolution of individual cross-peaks (Figure 1a), whereas FMA utilizes all peaks at a single mixing time (Figure 1b). Theoretically, FMA needs only one spectrum at an arbitrary mixing time. However, in the presence of noise the errors are close to minimum only in a limited mixing time interval.[19,25,26] Since the width and position of the interval is not known in advance, several experiments in a broad range of mixing times are needed. Thus, both BU and FMA require a set of exchange spectra at different mixing times. For peak volume normalization, FMA requires an exchange spectrum at zero mixing time as well. The principal weakness of BU analysis is that it ignores the correlations among the cross-peaks within individual 2D spectra (Figure 1a). The calculation of one buildup curve ignores the properties of all other buildup curves. Similarly, the FMA ignores the known dependence of cross peaks on time evolution; the FMA at one mixing time is independent from the FMA at any other mixing time (Figure 1b). A superior method shall use all available correlations within and among the spectra (Figure 1c) and shall minimize the random errors in a least-squares manner. Here we present a method that satisfies these requirements: a least error matrix analysis (LEMA). It provides the best estimates of magnetization exchange rate constants and their errors, using in a least-squares sense the information from a series of 2D spectra

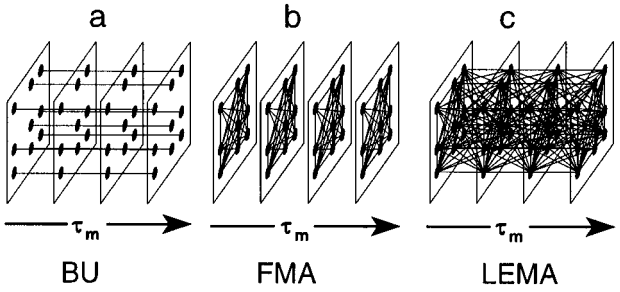

Figure 1. Schematic representation of the connectivities used in different methods for quantification of a series of 2D exchange spectra: (a) Buildup analysis (BU) uses the time evolution of individual cross peaks ignoring their connectivities within the spectra. (b) Full-matrix analysis (FMA) takes into account the connectivities among the peaks within a 2D spectrum but ignores the time evolution of peaks. (c) Least-errors matrix analysis (LEMA) uses all available correlations. It exploits the connectivities within a spectrum as FMA and the connectivities over mixing time as BU.

[†] On leave from Mathematical Institute, Knez Mihailova 35, Beograd, Yugoslavia.

* To whom correspondence should be addressed.

[⊗] Abstract published in *Advance ACS Abstracts,* May 1, 1997.

S1089-5639(96)03956-4 CCC: $14.00

recorded at different mixing times. We demonstrate its use and properties on a model dipeptide system, omitting the derivation of formulas.

Least Error Matrix Analysis (LEMA)

The spectral matrix of peak volumes $\boldsymbol{A}(\tau_m)$ at mixing time τ_m is related to the dynamic matrix $\boldsymbol{L}$ by[6]

$$\boldsymbol{A}(\tau_m) = \exp(-L\tau_m)\boldsymbol{A}(0) \tag{1}$$

from where

$$\boldsymbol{L} = -\ln(\boldsymbol{A}(\tau_m)\,\boldsymbol{A}(0)^{-1})/\tau_m \tag{2}$$

From a set of dynamic matrices $\boldsymbol{L}_k$ obtained using eq 2, the best values of magnetization exchange rate constants $[\boldsymbol{L}]_{pq}$ are found by iterative least-squares method:

$$[\boldsymbol{L}^{(i+1)}]_{pq} = \sum_k \frac{[\boldsymbol{L}_k]_{pq}}{[\sigma_k^{(i)}]_{pq}^2} \Big/ \sum_k \frac{1}{[\sigma_k^{(i)}]_{pq}^2} \tag{3}$$

where $[\boldsymbol{L}_k]_{pq}$ is the magnetization exchange rate constant for the (p,q)th spin pair obtained by FMA from the kth spectrum and, $\sigma_k^{(i)}$ is the propagated error calculated as[26]

$$\sigma_k^{(i)} = \begin{cases} \sigma(\tau_{m_k}, \boldsymbol{L}_k, \Delta A_{norm}), & i = 0 \\ \sigma(\tau_{m_k}, \boldsymbol{L}^{(i)}, \Delta \boldsymbol{A}_{norm}), & i > 0 \end{cases} \tag{4}$$

where $\Delta\boldsymbol{A}_{norm}$ is the matrix of peak volume errors, and $\boldsymbol{L}^{(i)}$ is the ith approximation of the dynamic matrix. The subscript norm indicates that the volume errors are normalized, i.e., expressed as a fraction of the volume of a diagonal peak (from the spin site with unit population) at zero mixing time. As a generalization of the case of equal random errors and equal spin populations,[26] the propagation of errors in a system with arbitrary spin populations and arbitrary uncorrelated volume errors is described by

$$[\sigma(\tau_m, \boldsymbol{L}, \Delta\boldsymbol{A}_{norm})]_{pq} \approx \left[\sum_{k,r,s,l} (n_p \nu_{pr} \nu_{rk}^T n_l \nu_{ls} \nu_{sq}^T)^2 \left((1 - \delta_{\lambda_r\lambda_s}) \left(\frac{\lambda_r - \lambda_s}{e^{-\lambda_r\tau_m} - e^{-\lambda_s\tau_m}} \right)^2 + \delta_{\lambda_r\lambda_s} \left(\frac{e^{\lambda_r\tau_m}}{\tau_m} \right)^2 \right) [\Delta\boldsymbol{A}_{norm}]_{kl}^2 \right]^{1/2} \tag{5}$$

The indexes in quadruple summation traverse the elements of volume error matrix $\Delta\boldsymbol{A}_{norm}$, and the eigenvalues λ and left eigenvectors ν of $\boldsymbol{L}$; n_p denotes the number of spins at pth spin site. The uncertainties in the magnetization exchange rates are given by[29]

$$[\Delta\boldsymbol{L}^{(i+1)}]_{pq} = 1/\sqrt{\sum_k \frac{1}{[\sigma_k^{(i)}]_{pq}^2}} \tag{6}$$

Since the error limits depend on the calculated dynamic matrix $\boldsymbol{L}$, and in return, the average value of $\boldsymbol{L}$ depends on the error limits, eqs 3−6 must be used in an iterative manner. For the first iteration, a subset of $\boldsymbol{L}_k$ that corresponds to nonextreme mixing times is used. In absence of crude errors, $\boldsymbol{L}^{(i)}$ converges toward the final value $\boldsymbol{L}$ usually after two iterations. The final $\boldsymbol{L}$ is the best ensemble average for a given set of 2D experiments. The particular FMA calculations (performed once for each spectral matrix) provide information about relations at a given mixing time, while the weights $[\sigma_k^{(i)}]_{pq}^2$ enforce the relationship among the cross peaks at different mixing times (Figure 1c).

SCHEME 1

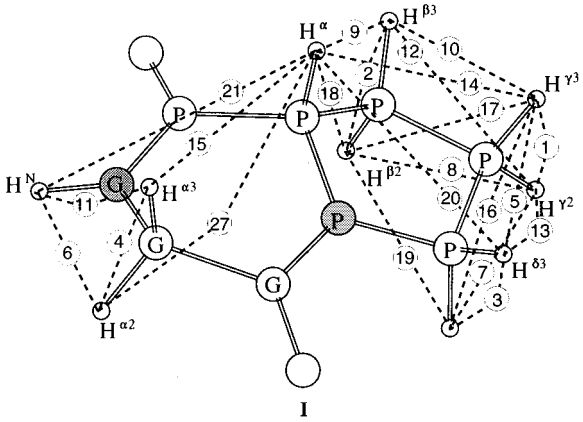

I

The least-squares minimization of random errors is accomplished by eq 3 that represents the standard expression for weighted averaging of a set of independent measurements.[29] Thus, LEMA provides statistically the best estimate for the dynamic matrix (eq 3) and its error limits (eq 6) from a set of independently determined matrixes at different mixing times.

Materials and Methods

To demonstrate the usefulness of LEMA, we have chosen a ten spin system, cyclo-(L-Pro-Gly) (**I**) (Scheme 1) in 3:1 v/v mixture H_2O/DMSO. At 233 K the dipeptide's cross-relaxation rates are between 0.001 and 10 s^{-1}, as for small proteins. At low temperatures the molecule is apparently rigid and most likely tumbles isotropically. A series of 2D exchange spectra (NOESY) has been recorded at 233 K on a Bruker AMX 500 spectrometer, with mixing times 0.000 06, 0.01, 0.02, 0.03, 0.04, 0.08, 0.16, 0.32, 0.64, and 1.28 s. The spectral data were processed using the Felix 95 (MSI Inc., San Diego, CA) software package. The peak volumes were determined by direct integration. Because of the severe spectral overlap between Pro $H^{\beta 2}$ and Pro $H^{\gamma 3}$ their peak volumes were measured together, and the respective component volumes were separated by the hybrid matrix approach using the known crystal structure.[30] The proton positions were optimized upon their attachment to heavy atoms in the crystal structure, by combined steepest descent and adopted basis Newton−Raphson method using the Charmm/Quanta (MSI Inc., San Diego, CA) software package. Also, we carried out a molecular dynamics (MD) simulation in vacuo and minimized the structure obtained after a 1 ns run. Comparing the two models (X-ray and molecular dynamics), we have estimated an average uncertainty in the geminal interproton distances at $2\sigma = 0.025$ Å, that translated into 8% relative error in the model cross-relaxation rates. Similarly, the errors for other proton pairs are estimated as $2\sigma = 0.1$ Å for distances below 3 Å and $2\sigma = 0.2$ Å for others. As a model geometry we have used the average distances from the X-ray and MD structure. The best agreement between the experimental and the model values for cross-relaxation rates of geminal proton pairs were found for $\tau_c = 3.8 \pm 0.2$ ns. For symmetric cross peaks, the volume errors ΔV were determined from the difference of volume integrals and were estimated as $\Delta V/V = 2\sigma_r = 4.8\%$ of the current peak volume. Also, an additive error (due to random noise) is estimated as $2\sigma_{norm} = 0.1\%$ of the diagonal line at $\tau_m = 0$. For the diagonal lines the errors were estimated as the deviation of the sum (diagonal + descendant cross-peaks) from a monoexponential decay. We express the error limits by 2 standard deviations, since $\pm 2\sigma$ represents the error interval with 95% probability. Then, in a set of 22 measured distances, only one distance is expected to deviate more than $\pm 2\sigma$ from the model value. The calculations were

TABLE 1: Comparison of LEMA and FMA ($\tau_m = 0.03$ s) Cross-Relaxation Rates and Interproton Distances in cyclo-(L-Pro-Gly) (Errors Are 2 Standard Deviations, $\Delta = 2\sigma$)

index[a]	spin pair	$-L_{mx}$[b]/ s^{-1}	$+\Delta L_{mx}$[c]/ s^{-1}	$-\Delta L_{mx}$[c]/ s^{-1}	$-L_{LEMA}$[d]/ s^{-1}	ΔL_{LEMA}[e]/ s^{-1}	$-L_{FMA}$[f]/ s^{-1}	ΔL_{FMA}[g]/ s^{-1}	r_{mx}[h]/ Å	Δr_{mx}/ Å	r_{LEMA}/ Å	$+\Delta r_{LEMA}$/ Å	$-\Delta r_{LEMA}$/ Å	r_{FMA}/ Å	$+\Delta r_{FMA}$/ Å	$-\Delta r_{FMA}$/ Å
1	$ProH^{\gamma 3}-ProH^{\gamma 2}$	7.32	0.60	0.66	6.13	0.61	6.69	1.58	1.76	0.025[i]	1.81	0.03	0.03	1.78	0.08	0.06
4	$GlyH^{\alpha 3}-GlyH^{\alpha 2}$	6.93	0.56	0.62	7.57	0.63	7.83	1.64	1.77	0.025[i]	1.75	0.02	0.02	1.74	0.07	0.05
6	$GlyH^{N}-GlyH^{\alpha 2}$	1.28	0.28	0.38	1.53	0.21	1.58	0.51	2.35	0.10	2.28	0.06	0.05	2.27	0.15	0.10
9	$ProH^{\alpha}-ProH^{\beta 3}$	1.14	0.25	0.33	1.19	0.16	1.19	0.45	2.40	0.10	2.38	0.06	0.05	2.38	0.20	0.12
13	$ProH^{\gamma 2}-ProH^{\delta 3}$	0.45	0.08	0.11	0.46	0.34	0.34	0.34	2.80	0.10	2.79	0.70	0.25	2.93	∞	0.51
14	$ProH^{\alpha}-ProH^{\gamma 3}$	0.41	0.08	0.10	0.57	0.14	0.59	0.23	2.84	0.10	2.69	0.13	0.10	2.67	0.23	0.14
15	$ProH^{\alpha}-GlyH^{\alpha 3}$	0.32	0.06	0.07	0.21	0.11	0.14	0.14	2.95	0.10	3.19	0.43	0.22	3.40	∞	0.82
20	$ProH^{\alpha}-ProH^{\delta 3}$	0.14	0.04	0.06	0.14	0.10	0.055	0.054	3.39	0.20	3.40	0.85	0.30	3.97	∞	1.02
21	$ProH^{\alpha}-GlyH^{N}$	0.069	0.018	0.026	0.11	0.08	0.15	0.15	3.82	0.20	3.52	0.82	0.30	3.35	∞	0.49
22	$ProH^{\alpha}-ProH^{\gamma 2}$	0.064	0.017	0.024	0.054	0.053	0.13	0.12	3.87	0.20	4.00	∞	0.63	3.46	∞	0.59
27	$ProH^{\alpha}-GlyH^{\alpha 2}$	0.042	0.010	0.015	0.11	0.10	0.064	0.062	4.14	0.20	3.56	2.79	0.38	3.87	∞	1.05

[a] Ordinal number in Figure 2. [b] Cross-relaxation rates from hybrid model (X-ray and molecular dynamics). [c] L_{mx}'s are calculated from the model V_{mx}'s which have symmetric error limits. Due to finite Δr's, the cross-relaxation error limits are asymmetric. [d] Cross-relaxation rates calculated from a series of NOESY spectra ($\tau_m = 0.000\,06$, 0.01, 0.02, 0.03, 0.04, 0.08, 0.16, 0.32, 0.64, and 1.28 s) by LEMA (eq 3). [e] Error limits from eq 6. [f] Cross-relaxation rates calculated by FMA (eq 2) from NOESY at $\tau_m = 0.03$ s. [g] Error limits from eq 5. [h] Interproton distances from a "hybrid" model: the average of the respective distances from the X-ray structure and from minimized MD structure. [i] For geminal pairs, the error limits were estimated by comparing the interproton distances in X-ray and MD models; a similar estimate ($2\sigma = 0.025$) is obtained from uncertainty in $C^{\alpha}-H$ distance in high-resolution neutron diffraction structures of amino acids.[33] There, it was found that the $C^{\alpha}-H$ distance varies ±0.008 Å due to the weak hydrogen bonding. Assuming that the HCH angle is constant, the uncertainty in r_{CH} of 0.008 Å propagates into r_{HH} as $2\sigma_{HH} = 0.025$ Å.

performed in Matlab 4.2c (Mathworks Inc.) software package on a Silicon Graphics Indigo2 computer (SGI Inc.). The Matlab implementation of LEMA is available from authors by email request (zsolt@mayo.edu).

Experimental Example: Cross-Relaxation in cyclo-(L-Pro-Gly) at 233 K

The cumulative experimental results are presented in Figure 2, and for a set of representative spin pairs more details are shown in Table 1. Figure 2a shows the experimental magnetization exchange rates calculated by LEMA (filled squares and thick error bars) and by FMA (thin error bars), in comparison with the model values (open rectangles). For clarity, the average values from FMA calculations are not shown. To emphasize the importance of their dynamic range, the cross-relaxation rates are plotted on a logarithmic scale. Figure 2b shows the respective interproton distances. In both figures, the values are sorted according to the model distances. The longest 15 interproton distances ($r > 5.2$ Å) are not shown because their cross-relaxation rates are too low to be deduced from the present experiments.

As is evident from Figure 2, the two sets of experimental values obtained using LEMA and FMA agree with the model within two standard deviations. However, the LEMA error limits are always narrower than the corresponding FMA limits. This is an obvious consequence of the ensemble-averaging property of LEMA in comparison to FMA. An important implication of such error reduction is that many cross-relaxation rates that cannot be determined from single FMA can be accurately determined by LEMA. That is the case with cross-relaxation rates 13, 15−18, 20, 21, and 27 in Figure 2 and Table 1. In FMA, the lower bond of estimated cross-relaxation rate errors becomes zero, which in return yields no upper limit for the corresponding interproton distance.

For interproton distances above 4 Å both methods fail to provide the cross-relaxation rates with a reasonable lower bond, with one exception in LEMA. In both cases, the upper error limits and the average cross-relaxation rates level off at approximately -0.1 s^{-1}. This is due to the fact that their cross peaks do not show up above the noise level even at the longest mixing time for which FMA does not fail. At the longer mixing times, when such peaks may have intensity above the noise level, the intensity of cross-peaks for the fastest process becomes equal to the intensities of the respective diagonal peaks within the limits of integration errors. Then, FMA fails,[26,31] being unable to produce any result[23] or yielding a completely different cross-relaxation matrix.[32] Thus, the lower limits for the accessible cross-relaxation rates (and the upper limit of the accessible distances) are determined by the longest mixing time and by the smallest peak volume that can be integrated. The longest mixing time is determined by the fastest exchange process. The smallest volume that can be integrated with a reasonable error is determined mostly by the signal-to-noise ratio. In present experiments, the range in which the magnetization exchange rates can be measured spans 2 orders of magnitude: from -7 s^{-1} for a distance of 1.75 Å to 0.07 s^{-1} for 4 Å. For measurements of interproton distances up to 5 Å, it would be necessary to measure the cross-relaxation rates as low as 0.01 s^{-1}. This can be achieved either by increasing the signal-to-noise ratio or by eliminating the fastest exchange process, the cross-relaxation among geminal spin pairs.

Another important property of magnetization exchange measurement that can be noticed from Figure 2 is a complete lack of correlation between the cross-relaxation rates (interproton distances) and their errors. This is a consequence of the fact that the spin diffusion is equally efficient in propagating errors as in transferring magnetization from one spin to the other.[26] Thus, for a given spin pair, the error is much larger in the presence of other spins. For example, the distances in spin pairs 13 (Pro $H^{\gamma 2}-$Pro $H^{\delta 3}$) and 14 (Pro $H^{\alpha}-$Pro $H^{\gamma 3}$) are approximately the same 2.80 vs 2.84 Å, but due to the relative isolation of Pro H^{α} proton, the distance error for the second pair is over 5 times smaller, 0.13 vs 0.7 Å (Table 1).

Also worth noticing is that all pairs which are well connected through the network have commensurate absolute errors irrespectively of the values of $[\boldsymbol{L}]_{pq}$. An important consequence is that in the presence of fast processes (large $[\boldsymbol{L}]_{pq}$) the slow processes (small $[\boldsymbol{L}]_{pq}$) cannot be satisfactorily quantified. This is even more obvious when the $[\boldsymbol{L}]_{pq}$ values are converted into interproton distances. Thus, even a modest improvement of the error limits for small $[\boldsymbol{L}]_{pq}$'s may have an immense effect on the upper error limits of the derived distances. In the structure determination, the reduction of error limits of the cross-relaxation rate constants facilitated by LEMA significantly improves the quality of geometrical input. Similarly, in a study of systems with chemical exchange, LEMA provides the best estimate of the chemical exchange rate constants from a given set of experimental data.

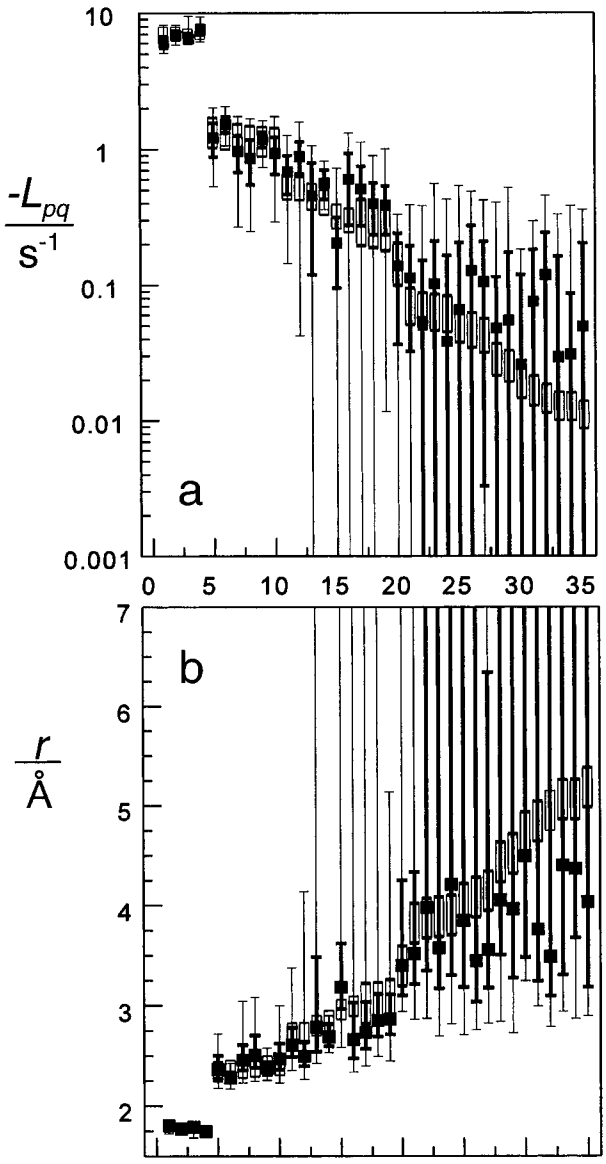

Figure 2. Cross-relaxation rates (a) and interproton distances (b) in cyclo-(L-Pro-Gly) obtained by LEMA from a series of 2D exchange spectra (filled squares). The thick error limits are from LEMA and the thin ones from FMA at 0.03 s. Due to averaging, the LEMA error limits are always narrower. When the cross-relaxation rates are converted into distances (isotropic motion, $\tau_c = 3.8$ ns, $\omega_0/2\pi = 500$ MHz) the improvement by LEMA is even more pronounced since the upper limits of the distances are determined by the lower limits of the cross-relaxation rates. The longest 15 interproton distances (not shown) cannot be determined because their upper limits tend to infinity (the lower bound of their respective cross-relaxation rates is zero). The open rectangles represents the 2σ ranges of the cross-relaxation rates and interproton distances derived from a hybrid model (the average of X-ray and MD distances). The upper and lower limits of the experimental interproton distances are not symmetric regarding the average distance because of finite errors in the corresponding cross-relaxation rates. Also, the magnitude of the errors (in both cross-relaxation rates and the interproton distances) is not proportional to the respective mean values due to the influence of the structure of dynamic matrix on the absolute error.

Conclusion

In conclusion, we have proposed a least-squares method for matrix analysis, LEMA, that provides the best estimate of the dynamic matrix by weight averaging the dynamic matrices determined at different mixing times. We have shown that the high precision analysis of dynamic systems (chemical exchange and cross-relaxation) studied by 2D exchange spectroscopy is possible only from a series of 2D experiments recorded at different mixing times. The accuracy of the deduced dynamic matrices (chemical exchange or cross-relaxation) is determined by the range of the measured magnetization exchange rate constants and by the accuracy of peak volume integrals. Ultimately, both are governed by the signal-to-noise ratio of the volume integrals. An unavoidable practical limitation is that, in principle, the slow processes (in both EXSY and NOESY) cannot be well quantified in the presence of fast ones. However, as we have experimentally demonstrated, LEMA can extend the lower limit of magnetization exchange rate constants for an order of magnitude in comparison to the individual FMA of the same data set.

Acknowledgment. We thank Dr. Nigel J. Clarke for a critical reading of the manuscript.

References and Notes

(1) Jeener, J.; Meier, B. H.; Bachmann, P.; Ernst, R. R. *J. Chem. Phys.* **1979**, *71*, 4546−4553.
(2) Ernst, R. R.; Bodenhausen, G.; Wokaun, A. *Principles of Nuclear Magnetic Resonance in One and Two Dimensions*; Oxford University Press: New York, 1987.
(3) Meier, B. H.; Ernst, R. R. *J. Am. Chem. Soc.* **1979**, *101*, 6441−6442.
(4) Huang, Y.; Macura, S.; Ernst, R. R. *J. Am. Chem. Soc.* **1981**, *103*, 5327−5333.
(5) Kumar, A.; Ernst, R. R.; Wüthrich, K. *Biochem. Biophys. Res. Commun.* **1980**, *95*, 1−6.
(6) Macura, S.; Ernst, R. R. *Mol. Phys.* **1980**, *41*, 95−117.
(7) Wüthrich, K. *NMR of Proteins and Nucleic Acids*; John Wiley & Sons: New York, 1986.
(8) Bremer, J.; Mendz, G. L.; Moore, W. J. *J. Am. Chem. Soc.* **1984**, *106*, 4691−4696.
(9) Denk, W.; Baumann, R.; Wagner, G. *J. Magn. Reson.* **1986**, *67*, 386−390.
(10) Broido, M. S.; James, T. L.; Zon, G.; Keepers, J. W. *Eur. J. Biochem.* **1985**, *150*, 117−128.
(11) Boelens, R.; Koning, T. M. G.; Kaptein, R. *J. Mol. Struct.* **1988**, *173*, 299−311.
(12) Holak, T. A.; Scarsdale, J. N.; Prestegard, J. H. *J. Magn. Reson.* **1987**, *74*, 546−549.
(13) Borgias, B. A.; James, T. L. *Methods Enzymol.* **1989**, *176*, 169−183.
(14) Madrid, M.; Jardetzky, O. *Biochim. Biophys. Acta* **1988**, *953*, 61−69.
(15) Kim, S.-G.; Reid, B. R. *J. Magn. Reson.* **1992**, *100*, 382−390.
(16) Liu, H.; Spielmann, P.; Ulyanov, N.; Wemmer, D.; James, T. *J. Biomol. NMR* **1995**, *6*, 390−402.
(17) Mendz, G. L.; Robinson, G.; Kuchel, P. W. *J. Am. Chem. Soc.* **1986**, *108*, 169−173.
(18) Abel, E. W.; Coston, T. P. J.; Orrell, K. G.; Sik, V.; Stephenson, D. *J. Magn. Reson.* **1986**, *70*, 34−53.
(19) Perrin, C. L. *J. Magn. Reson.* **1989**, *82*, 619−621.
(20) Willem, R. *Prog. NMR Spectrosc.* **1987**, *20*, 1−94.
(21) Perrin, C. L.; Dwyer, T. J. *Chem. Rev.* **1990**, *90*, 935−967.
(22) Landy, S. B.; Rao, B. D. N. *J. Magn. Reson.* **1989**, *83*, 29−43.
(23) Post, C. B.; Meadows, R. P.; Gorenstein, D. G. *J. Am. Chem. Soc.* **1990**, *112*, 6796−6803.
(24) Landy, S. B.; Rao, B. D. N. *J. Magn. Reson.* **1993**, *B102*, 209−213.
(25) Macura, S. *J. Magn. Reson.* **1994**, *B104*, 168−171.
(26) Macura, S. *J. Magn. Reson.* **1995**, *112*, 152−159.
(27) Schwerk, U.; Michel, D. *J. Phys. Chem.* **1996**, *100*, 352−356.
(28) Macura, S.; Farmer, B. T. II; Brown, L. R. *J. Magn. Reson.* **1986**, *70*, 493−499.
(29) Bevington, P. R. *Data Reduction and Error Analysis for the Physical Sciences*; McGraw-Hill: New York, 1969.
(30) Von Dreele, R. B. *Acta Crystallogr.* **1975**, LB31, 966−970.
(31) Macura, S.; Fejzo, J.; Westler, W. M.; Markley, J. L. *Bull. Magn. Reson.* **1994**, *16*, 73−93.
(32) Zolnai, Z.; Juranić, N.; Macura, S., submitted.
(33) Steiner, T. *J. Chem. Soc.* **1995**, *2*, 1315−1319.